research papers

**Lucas Rodríguez Pirani,[a]
Mauricio F. Erben,[a]* Roland
Boese,[b] C. Gustavo Pozzi,[c]
Adolfo C. Fantoni[c] and Carlos O.
Della Védova[a,d]***

[a]CEQUINOR (UNLP-CONICET CCT La Plata),
Departamento de Química, Facultad de Cien-
cias Exactas, Universidad Nacional de La Plata,
47 esq. 115 (B1900AJL), CC 962, La Plata,
Buenos Aires, Argentina, [b]Institut für Anorga-
nische Chemie, Universität Duisburg-Essen,
Universitätsstrasse 5-7, D-45117 Essen,
Germany, [c]Instituto de Física La Plata, Departa-
mento de Física, Facultad de Ciencias Exactas,
Universidad Nacional de La Plata, 49 y 115, La
Plata, Buenos Aires, Argentina, and [d]Laboratorio
de Servicios a la Industria y al Sistema Científico
(UNLP-CIC-CONICET), Camino Centenario,
Gonnet, Buenos Aires, Argentina

Correspondence e-mail:
erben@quimica.unlp.edu.ar,
carlosdv@quimica.unlp.edu.ar

Conformational preference of chlorothioformate species: molecular structure of ethyl chlorothioformate, ClC(O)SCH₂CH₃, in the solid phase and NBO analysis

The molecular structure of ethyl chlorothioformate, $ClC(O)SCH_2CH_3$, has been investigated in the solid phase by X-ray diffraction analysis at low temperature using a miniature zone-melting procedure and IR laser radiation. The crystalline solid consists exclusively of molecules with the *synperiplanar* conformation with respect to the C=O double bond and the S—C single bond, and *gauche* orientation of the ethyl group (*syn-gauche*). These results coincide with previous studies devoted to gas-phase conformational properties. The conformational preference for the $ClC(O)SY$ (Y = Cl, CF_3, CH_3 and CH_2CH_3) series of molecules was rationalized using the natural bond orbital (NBO) scheme. It was found that both resonance (mesomeric) and anomeric (hyperconjuga-tion) intermolecular charge-transfer interactions are impor-tant for describing the *syn* ↔ *anti* equilibrium, also illustrating the effect of electronegativity of the substituent in the conformation preference of the $ClC(O)S-$ moiety. On the basis of the atoms in molecules (AIM) theory, intermolecular interactions have been characterized in the B3LYP/6-31G** periodic boundary electron density.

1. Introduction

Thiochemicals are sulfur analogs of oxygen-containing compounds; for example, thiochemicals containing sulfur in the +2 oxidation state, mercaptans and alkyl sulfides are sulfur analogs of alcohols and ethers (Yen *et al.*, 2005). In this context a comparison of chemical reactivity as well as the structural and conformational properties of oxoesters and thioesters of the type $XC(O)EY$ (E = O, S) have been extensively analyzed. Differences between these compounds could display a key role in biological systems, such as coenzyme A (Stryer, 1995; Yang & Drueckhammer, 2001). Structural and conformational investigations on simple sulfur and oxygen analogs were performed including the compounds $ClC(O)ECF_3$ (Gobbato *et al.*, 1997; Erben *et al.*, 2004), $CH_3C(O)EC(O)CH_3$ (Romano *et al.*, 2001; Vledder *et al.*, 1971) and $ClC(O)ECH_3$ (Durig & Griffin, 1977; O'Gorman *et al.*, 1950; Shen *et al.*, 1995; Romano *et al.*, 2004). The essentially planar structure around the $-C(O)E-$ (E = O, S) skeletons gives rise to *syn* [τ(O=CEY) = 0°] and *anti* [τ(O=CEY) = 180°] conformational options (see Fig. 1).

An increasingly rich conformational behavior arose from the linking of a second group to the $-C(O)E-$ moiety. Thus ethyl oxo- and thioesters, of the general formula $XC(O)ECH_2CH_3$ (with X = H, Cl, F, CN, CF_3), can adopt, along with the *syn* and *anti* conformations described above, different C—E—C—C dihedral angles. The main forms are the *gauche* [τ(CECC) = 90°] and *anti* [τ(CECC) = 180°] conformations. These systems have been exhaustively studied

nearly 30 years ago by True and Bohn using low-resolution microwave spectroscopy. These investigations were also performed on the basis of a comparison with the analogous oxoesters, which showed similar conformational properties, although some remarkable differences were observed. Thus, microwave spectra of ethyl formate (Riveros & Wilson, 1967) and ethyl fluoroformate, chloroformate, cyanoformate and trifluoroacetate (True & Bohn, 1976) were interpreted in terms of a mixture of conformers which have a *syn* conformation of the O=C—O—C dihedral angle coupled with *gauche* or *anti* conformations about the C—O—C—C dihedral angle. Among the ethyl thioester analogs, ethyl fluorothioformate and chlorothioformate also display both *syn-gauche* and *syn-anti* conformations like the oxoesters (True *et al.*, 1981; Bohn & Wiberg, 1999). On the other hand, the microwave spectra of ethyl cyanothioformate and trifluorothioacetate display only the *syn-gauche* conformer at ambient temperature (True *et al.*, 1981). Nevertheless, a gas electron-diffraction study on $CF_3C(O)SCH_2CH_3$ has very recently demonstrated that both *syn-gauche* and *syn-anti* conformers are present in equilibrium (Lestard *et al.*, 2009).

Taking into account these antecedents, at least three conformations, *i.e.* the *syn-gauche*, *syn-anti* and *anti-gauche* forms, may be expected for the title species. These conformers are shown in Fig. 2.

Since simple thioester compounds are usually liquids at ambient temperatures, rather little information is known about their structural behavior in the solid state. Only with the development of special crystallization techniques applicable to compounds that are liquids or gases at normal temperatures has it been possible to extend detailed structural studies to the crystalline state (Romano *et al.*, 1999, 2003). For example, the compounds $FC(O)SSC(O)CF_3$ (Erben *et al.*, 2005) and $CH_3OC(O)SNCO$ (Vallejos *et al.*, 2007) have been recently
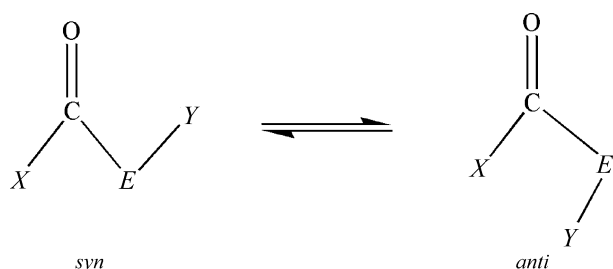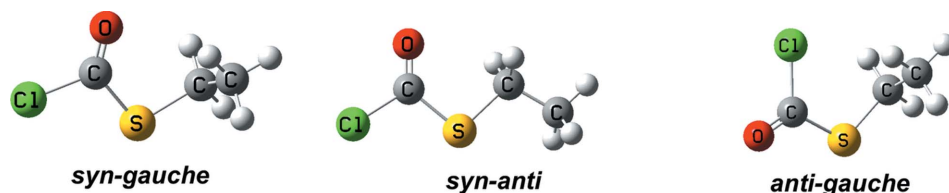
investigated using this method. While both compounds exist as an equilibrium mixture of the *syn* and *anti* conformers in the liquid and gas phases, only the *syn* rotamer has been observed in each of the crystals at *ca* 170 K. A similar picture emerges from the study of $CF_2ClC(O)SH$ (Erben *et al.*, 2007), which consists exclusively of molecules adopting a *syn* conformation, favoring the formation of cyclic dimers in the crystal through S—H···O=C hydrogen bonds.

Of central interest for the present work are previous conformational studies on *O*- and *S*-ethyl chloro-(thio)formates based on a combination of matrix isolation IR spectroscopy and quantum chemical calculations. The planar *syn-anti* form of $ClC(O)OCH_2CH_3$ is slightly more stable than the *syn-gauche* conformer, the conformational ratio in the gas phase at room temperature being 62:38 (Tobón *et al.*, 2008). The existence of the two equivalent conformers in the liquid and gas phases was also proposed for the thioformate $ClC(O)SCH_2CH_3$ species. However, the conformational equilibrium is inverted, with the most stable conformer being the *syn-gauche* form, with the *syn-anti* form higher in energy by 1.26 kJ mol^{-1} (0.30 kcal mol^{-1}; True *et al.*, 1981).

The rich conformational behavior displayed by these species in the vapor and liquid phases and in the presence of several conformers within a narrow energy range encouraged us to extend the study to the crystalline phase. In this work the molecular and crystal structure of *S*-ethyl chlorothioformate has been determined by X-ray diffraction analysis at low temperature using a miniature zone-melting procedure. In order to characterize the intermolecular interactions at play, the topology of the electron density obtained from a periodic quantum calculation was analyzed within the context of Bader's theory of atoms in molecules (Bader, 1990; Popelier, 2000; Matta & Boyd, 2007). Moreover, an NBO population analysis has been performed with the primary aim of deepening the understanding of how electronic interactions affect the conformational behavior in thioester species.

2. Experimental

Chlorothioformates are useful intermediates for the production of herbicidal thiocarbamates and similar compounds. Ordinary thiocarbamates were readily obtained from the reaction of the appropriate amine with ethyl chlorothioformate (Sitzmann & Gilligan, 1985). Small alkyl chlorothioformates are prepared by the reaction of thiophosgene with a potassium alkoxide (Zaim, 1999) and improved methods have been reported (Fiske *et al.*, 2006). Moreover, the hydrolysis (Castro *et al.*, 2006) and solvolysis (Kevill & D'Souza, 1998) of alkyl chlorothioformates have also been studied.

To avoid the use of chloroformate and thiophosgene reagents, *S*-ethyl chlorothioformate was synthesized using triphosgene and ethanethiol in the presence of tri-

Figure 1
Conformational equilibrium around the C(O)—*E* bond for *XC*(O)*EY* molecules.

Figure 2
Stable conformers of $ClC(O)SCH_2CH_3$ in the gas phase.

Lucas Rodríguez Pirani *et al.* · Conformational preference of chlorothioformate species

Table 1
Experimental details.

Crystal data	
Chemical formula	C_3H_5ClOS
M_r	124.58
Cell setting, space group	Monoclinic, $P2_1/c$
Temperature (K)	183
a, b, c (Å)	9.4763 (6), 5.8288 (4), 11.0764 (7)
β (°)	112.853 (1)
V (Å^3)	563.79 (6)
Z	4
Radiation type	Mo $K\alpha$
μ (mm^{-1})	0.91
Crystal size (mm)	$0.3 \times 0.3 \times 0.3$
Data collection	
Diffractometer	Siemens SMART CCD area detector
Absorption correction	Multi-scan (Blessing, 1995)
T_{min}, T_{max}	0.93, 0.97
No. of measured, independent and observed [$I > 2\sigma(I)$] reflections	2014, 1241, 1182
R_{int}	0.013
Refinement	
$R[F^2 > 2\sigma(F^2)]$, $wR(F^2)$, S	0.018, 0.050, 1.07
No. of reflections	1241
No. of parameters	55
No. of restraints	0
H-atom treatment	H-atom parameters constrained
$\Delta\rho_{max}, \Delta\rho_{min}$ (e Å^{-3})	0.24, -0.15

ethylamine (Salomon & Breuer, 2000), according to the following equation.

$$Cl_3COC(O)OCCl_3 + 2CH_3CH_2SH \rightarrow$$
$$Cl_3COC(O)SCH_2CH_3 + ClC(O)SCH_2CH_3 + 2HCl \quad (1)$$
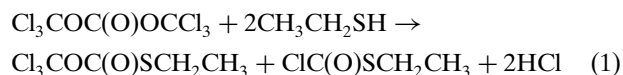
The liquid product was purified by fractional distillation and subsequently purified several times by fractional condensation at reduced pressure to eliminate volatile impurities. The final purity of the compound in both the vapor and liquid phases was carefully checked by IR (vapor) and Raman (liquid) (Ulic *et al.*, 1998).

A single crystal of *ca* 0.3 mm diameter was grown at a temperature of 183 K in a Pyrex capillary mounted on a Siemens SMART CCD diffractometer device using a miniature zone-melting procedure driven using IR laser radiation (Brodalla *et al.*, 1985). Intensities were collected using graphite-monochromated Mo $K\alpha$ radiation ($\lambda = 0.71073$ Å). Crystal data and data collection details are listed in Table 1.

The structure was solved from a Patterson synthesis and refined by full-matrix least-squares methods on F^2, with *SHELXTL-Plus* (Sheldrick, 2008). H atoms were included in idealized positions and treated with a riding model with 1.2-fold (1.5-fold for the methyl group) isotropic displacement parameters of the equivalent U_{iso} of the corresponding C atoms. All non-H atoms were refined with anisotropic displacement parameters. The final conventional R factor and weighted R factors, wR, are listed in Table 1.[1]

[1] Supplementary data for this paper are available from the IUCr electronic archives (Reference: PS5011). Services for accessing these data are described at the back of the journal.

Geometry optimization and frequency calculations for different conformers of $ClC(O)SCH_2CH_3$ were performed with the *GAUSSIAN*03 program package (Frisch *et al.*, 2004). MP2 and B3LYP methods were used employing standard basis sets up to the extended valence triple-ξ basis set augmented with diffuse and polarization functions for all atoms (6-311++G**). Natural population analysis and second-order donor → acceptor interaction energies were estimated at the B3LYP/6–311++G** level using the NBO analysis (Reed *et al.*, 1988) implemented in the *GAUSSIAN*03 program.

Periodic calculations were performed at the B3LYP/6-31G** level with *Crystal*98 (Saunders *et al.*, 1998) and *Crystal*09 (Dovesi *et al.*, 2005, 2009) codes. Using the experimental estimations as the starting point, the coordinates of the H atoms in the crystal were optimized to minimize the B3LYP/6-31G** crystal energy with heavy atom coordinates and cell parameters fixed at their experimental values. The topology of the resulting electron density was then analyzed using the *TOPOND*98 (Gatti, 1999) code.

3. Results and discussion

3.1. NBO analysis

Electronic interactions have been analyzed mainly through the evaluation of anomeric and mesomeric contributions (Kirby, 1983) with the primary aim of understanding the conformational properties of thioester compounds (Erben *et al.*, 2002; Kirby, 1983; Lestard *et al.*, 2009). Here an NBO population analysis has been carried out for the ClC(O)SY [Y = Cl (Shen & Hagen, 1985), CF$_3$ (Ulic *et al.*, 2002), CH$_3$ (Shen *et al.*, 1995) and CH$_2$CH$_3$] series of molecules, which are S-substituted chlorothioformates with experimentally available data for their molecular structure. Based on the previous study for related $-C(O)SCl$ species (Erben *et al.*, 2002), the lpπ(S) → π*C=O mesomeric interaction has been evaluated for *syn* ↔ *anti* conformational equilibrium (C=O double bond and S—Y single bond in mutual *syn* or *anti* conformations, see Fig. 1). The donor–acceptor energies involving the lpσ(S) → σ*C=O and lpσ(S) → σ*C—Cl interactions (anomeric effect) were taken into account for the *syn* and *anti* conformers. Table 2 lists the difference values for the donor–acceptor interaction energies computed at the B3LYP/6–311++G** level between the anomeric ($\Delta E_{anom} = E[$lpσ(S) → σ*C=O] − $E[$lpσ(S) → σ*C—Cl]) and mesomeric ($\Delta E_{mes} = E[$lpπ(S) → π*(C=O)]$_{syn}$ − $E[$lpπ(S) → π*(C=O)]$_{anti}$) interactions for each conformer. Clearly these values depend on the Y group attached to the S atom. In all cases both electronic effects tend to stabilize the *syn* conformer, in good agreement with the computed zero-point corrected electronic energy ($\Delta E°$).

It is noteworthy that both contributions are greater for R = CH$_3$ and CH$_2$CH$_3$ than for R = Cl or CF$_3$ (see Table 2). This behavior might be understood from the chemical nature of the substituents. In effect, electron density from the lone pairs formally localized on the S atom becomes more available when the electronegativity of the R group decreases, and this favors the donor capacity of the S atom.

Table 2
Stabilization energies (in kJ mol^{-1}) for orbital interactions between lp$_\pi$ and lp$_\sigma$ sulfur lone pairs and the π*(C=O), σ*(C=O) and σ*(C—Cl) acceptor orbitals computed for *syn* and *anti* conformers for ClC(O)SY compounds, and relative total energies obtained using the B3LYP/6-311++G** level of approximation.

The carbonyl bond distance [d(C=O)] and stretching frequency [$\nu_{C=O}$] are also given.

		ClC(O)SCl		ClC(O)SCF$_3$		ClC(O)SCH$_3$		ClC(O)SCH$_2$CH$_3$	
		syn	*anti*	*syn*	*anti*	*syn*	*anti*	*syn*	*anti*
lp$_\pi$(S) → π*(C=O)†		30.40	27.31	30.33	27.68	35.79	33.48	35.50	33.11
lp$_\sigma$(S) → σ*(C=O)‡		5.74	–	5.47	–	6.41	–	6.66	–
lp$_\sigma$(S) → σ*(C—Cl)‡		–	4.43	–	4.72	–	5.60	–	5.85
ΔE_{total}^{int}§		4.40		3.40		3.12		3.20	
ΔE¶		−2.91		−3.18		−2.92		−3.21	
d(C=O) (Å)	Calc.	1.177	1.187	1.179	1.183	1.186	1.184	1.186	1.184
	GED	1.183 (5)^a	–	1.177 (4)^b	–	1.191 (3)^c	–	–	–
	XRD	1.166 (8)^d	–	–	–	1.172 (2)^d	–	1.1810 (13)^e	–
	$\nu_{C=O}$ (cm^{-1})	1803^d	–	1801^f	–	1775^d	–	1770^g	–

References: (*a*) Shen & Hagen (1985), (*b*) Gobbato *et al.* (1997), (*c*) Shen *et al.* (1995), (*d*) Romano *et al.* (2003), (*e*) this work, (*f*) Ulic *et al.* (2002), (*g*) Ulic *et al.* (1998). † Mesomeric effect. ‡ Anomeric effect. § $\Delta E_{total}^{int} = \Delta E_{meso}^{int} + \Delta E_{anom}^{int}$, where ΔE_{meso}^{int} is the mesomeric interactions energy difference of the *syn* and *anti* conformers and ΔE_{anom}^{int} is the anomeric interactions energy difference of the *syn* and *anti* conformers. ¶ $\Delta E = E^{syn} - E^{anti}$ is the energy difference of the *syn* and *anti* conformers.

The mesomeric and anomeric interactions promoted by electron donation from the out-of-plane (π) and in-plane (σ) sulfur lone pairs directly affect the bond length of the carbonyl group, mainly in the *syn* conformer. A longer C=O bond distance is expected when the interaction between lone pairs and the antibonding orbital of carbonyl increases. As shown in Table 2, the experimental gas-phase carbonyl bond distance [d(C=O)] is longer for ClC(O)SCH$_3$ than ClC(O)SCl and ClC(O)SCF$_3$. Similarly, $\nu_{C=O}$ for alkyl-substituted species (Y = CH$_3$ and CH$_2$CH$_3$) lies in the 1770–1775 cm^{-1} region, whereas for Y = Cl and CF$_3$ $\nu_{C=O}$ is observed definitely above 1800 cm^{-1} in the gas-phase IR spectra. Both observations are in agreement with a higher population of the antibonding π*$_{C=O}$ orbital for ClC(O)SCH$_3$ and ClC(O)SCH$_2$CH$_3$, as deduced from the NBO analysis.

For the *syn* conformation, both mesomeric and anomeric effects influence the carbonyl group through electron donations to the π*$_{C=O}$ and σ*$_{C=O}$ antibonding orbitals. For the *anti* form, only the mesomeric interaction has a direct influence on this form, mainly because interactions between the lp$_\sigma$(S) with the C=O group are prevented by symmetry effects. This absence of anomeric interaction over the carbonyl group for the molecules with an *anti* conformation is in line with the near invariance observed in the C=O bond length for the *anti* conformers of the studies species (see theoretical values in Table 2).

These variations of the molecular structure when the electronegative nature of the X group is changed prompted us to investigate in more detail the molecular structure of ClC(O)SCH$_2$CH$_3$.

3.2. Crystal structure

A summary of the key crystallographic information for the title compound is given in Table 1. The molecular structure in

the solid state (see Fig. 3) more closely resembles the *syn-gauche* conformation, belonging to the C_1 symmetry point group, with torsion angles τ(CS—C=O) and τ(CS—CC) of −0.78 (13) and −84.73 (9)°. The main geometric parameters derived from the structure refinement are shown in Table 3, together with those obtained from quantum chemical calculations (B3LYP/6-311++G** and MP2/6-311++G**). These levels of calculation predict that the bond lengths and bond angles of the free molecule lie within 0.03 Å and 2° of those obtained in the solid phase, improving the theoretical description offered in our previous work (Ulic *et al.*, 1998).

Owing to their chemical similarity, the molecular structures of the related species ClC(O)SCl and ClC(O)SCH$_3$ in the solid phase (Shen *et al.*, 1995; Romano *et al.*, 2003) can be compared with ClC(O)SCH$_2$CH$_3$. Thus, with increasing electronegativity of the bonded atom the sulfur is expected to shrink in size as its negative charge decreases [*e.g.* in going from ClC(O)SCH$_2$CH$_3$ to ClC(O)SCl]. In this sense, in Table 3 we can observe that the C—S—C bond angle in ClC(O)SCH$_2$CH$_3$ is 1.4° smaller than the corresponding angle in ClC(O)SCl (C—S—Cl). Also, the O=C—S bond angle is contracted by 1.5° with respect to the same angle in ClC(O)SCl. The same behavior is also observed for the ClC(O)SCH$_3$ molecule, when the gas electron diffraction (GED) values obtained from the literature (Shen *et al.*, 1995) are compared. The differences around the O=C—S—Y moiety might be caused by the greater repulsive radii formally located in the lone-pair direction around sulfur when the Y group is less electronegative. This is not surprising because lone-pair electrons are expected to be more polarizable than bonding electrons. This concept concerning the effective radius in both lone-pair and bonding orbitals was very recently established by Gillespie in connection with the ligand close-packing model (Gillespie *et al.*, 2010).
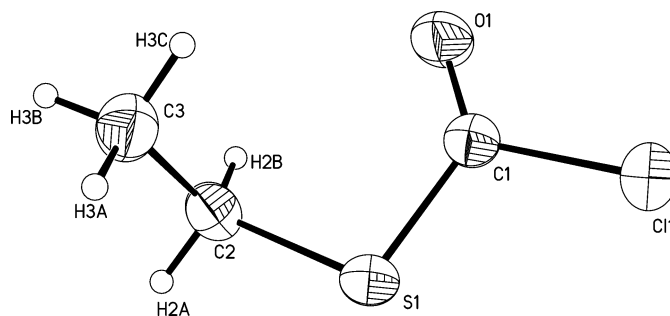

Figure 3
Molecular structure of ClC(O)SCH$_2$CH$_3$ in a single crystal.

Table 3
Experimental (X-ray) and calculated (B3LYP and MP2 methods with the 6-311++G** basis sets) geometric parameters for the *syn–gauche* conformer of ClC(O)SCH$_2$CH$_3$.

Reported values for the crystalline structure of the related species ClC(O)SCH$_3$ and ClC(O)SCl are also given.

Parameters†	Experimental‡	B3LYP	MP2	ClC(O)SCH$_3$§	ClC(O)SCl§
S—C1	1.733 (1)	1.763	1.750	1.723 (2)	1.740 (7)
S—C2/Cl	1.813 (1)	1.844	1.815	1.798 (2)	2.006 (3)
Cl—C	1.783 (1)	1.810	1.778	1.786 (2)	1.775 (7)
C=O	1.181 (1)	1.186	1.198	1.172 (2)	1.166 (8)
C2—C3	1.513 (2)	1.524	1.524	–	–
C—S—C/Cl	99.62 (5)	99.8	98.3	99.6 (1)	101.0 (2)
O=C—S	129.33 (9)	128.2	127.2	129.3 (2)	130.8 (6)
O=C—Cl	120.95 (9)	121.5	121.9	120.7 (2)	123.5
S—C—Cl	109.73 (5)	110.2	110.9	110.0 (1)	105.7 (4)
C—C—S	112.73 (8)	114.1	113.1	–	–
CS—C=O	−0.8 (1)	1.2	2.9	–	–
CS—CCl	179.01 (6)	−179.2	−177.4	–	–
CS—CC	−84.73 (9)	79.9	76.5	–	–

† For atom numbering see Fig. 3. ‡ Distance values in Å and bond angles in °. Uncertainties are σ values. § Taken from Romano *et al.* (1999).

Table 4
Topological properties of the intermolecular interactions in the B3LYP/6-31G** electron density of the ClC(O)SCH$_2$CH$_3$ crystal.

Internuclear distance (R, Å), electron density (ρ, e Å^{-3}), Laplacian ($\nabla^2\rho$, e Å^{-5}) and positive principal curvature (λ_3, e Å^{-5}) evaluated at the corresponding (3,−1) critical points.

Attractors†		R	ρ	$\nabla^2\rho$	λ_3
S	Cl^i	3.96	0.021	0.250	0.327
H$_{et}$	O^i	2.55	0.053	0.740	1.060
S	Cl^{ii}	3.84	0.022	0.290	0.366
Cl	Cl^{ii}	3.68	0.033	0.414	0.554
Cl	H$_{et}$^{iii}	3.05	0.030	0.364	0.525
Cl	O^{iii}	3.60	0.023	0.340	0.440
O	H$_{me}$^{iv}	3.04	0.029	0.390	0.476
Cl	C3^{iv}	3.74	0.022	0.287	0.320
H$_{me}$	H$_{me}$^{iv}	2.56	0.022	0.268	0.390
C2	S^v	4.12	0.015	0.168	0.207
H$_{et}$	Cl^v	2.96	0.038	0.458	0.673
C1	S^{vi}	3.69	0.031	0.327	0.394
Cl	S^{vi}	3.85	0.031	0.349	0.436
H$_{me}$	O^{vii}	2.72	0.035	0.461	0.682
H$_{me}$	H$_{me}$^{vii}	2.66	0.025	0.319	0.393
H$_{me}$	H$_{me}$^{viii}	2.77	0.026	0.325	0.400

Symmetry codes: (i) $x, 1+y, z$; (ii) $-x, \frac{1}{2}+y, \frac{1}{2}-z$; (iii) $x, -\frac{1}{2}-y, -\frac{1}{2}+z$; (iv) $-1-x, -\frac{1}{2}+y, \frac{1}{2}-z$; (v) $x, \frac{1}{2}-y, \frac{1}{2}$. † First column: reference molecule.

Bond lengths and angles in ClC(O)SCH$_2$CH$_3$ are very similar to those in ClC(O)SCH$_3$, while some interesting differences are observed with respect to ClC(O)SCl (see Table 3). Thus, the O=C—S and O=C—Cl bond angles are 1.5 and 2.5° higher in ClC(O)SCl than in the title molecule.

A schematic view of the crystal packing of ClC(O)SCH$_2$CH$_3$ is shown in Fig. 4.

3.3. Topology of the electron density

In AIM theory (Bader, 1990; Popelier, 2000; Matta & Boyd, 2007), (3,−1) critical points corresponding to closed-shell interactions are characterized by a low positive value of the Laplacian of the electron density ($\nabla^2\rho_c$) and a low value of the electron density (ρ_c). For this kind of interaction ρ_c can be used as an indicator of the interaction strength. However,
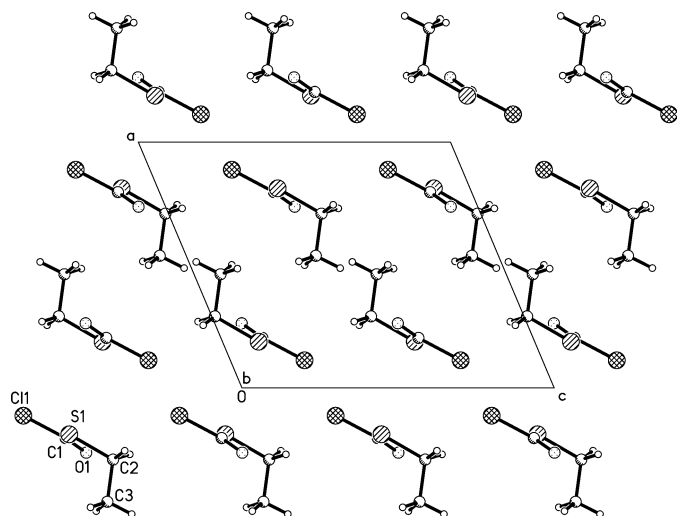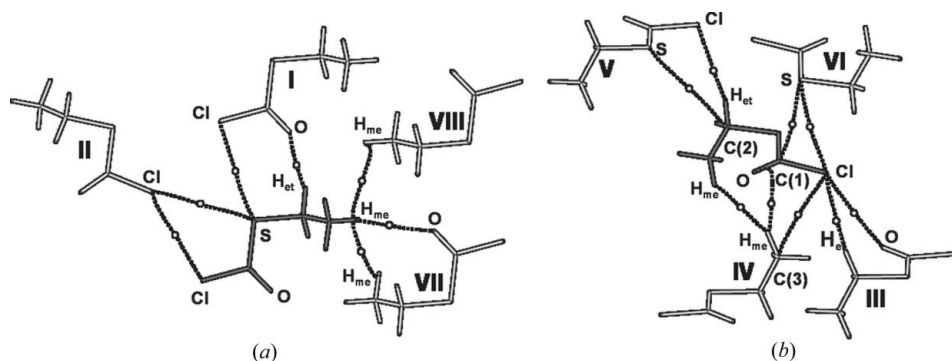

Figure 4
Two-dimensional illustration of the crystal packing of ClC(O)SCH$_2$CH$_3$.

when dealing with interactions that can be considered to be hydrogen bonds, λ_3, the positive eigenvalue of the Hessian of ρ, has been shown to correlate better with the interaction energies (Espinosa *et al.*, 1999).

Sixteen unique intermolecular (3,−1) critical points (ICPs) were located in the periodic electron density of the title compound. These bind a reference molecule to eight of its 13 nearest neighbors. The ICPs found in the eight unique molecular pairs and their associated bond paths (BPs) are shown in Fig. 5. Values for the parameters characterizing the ICPs are listed in Table 4, where labeling of the symmetry operations generating the pairs is also presented. As expected, in a general context intermolecular interactions vary in strength ranging from medium–weak to weak.

In relative terms, either considering ρ_c or λ_3, the strongest interaction is the hydrogen bond that links the carbonyl oxygen to one of the ethyl H atoms. The non-bonded distance involved (2.65 Å) is consistently only slightly shorter than the sum of the corresponding van der Waals radii. This kind of interaction has also been reported for the crystalline structure of ClC(O)SCH$_3$ (Romano *et al.*, 2003).

The structure features Cl···Cl interactions measuring 3.68 Å. Although this distance is longer than twice the van der Waals radius of chlorine (Bondi, 1964), the topological parameters suggest that the interaction is amongst the most stabilizing in the structure. The nature of short Cl···Cl contacts has long been a matter for discussion (Mirsky & Cohen, 1978; Sarma & Desiraju, 1986), but more recent interest (Desiraju, 2007; Nayak *et al.*, 2009; Hathwar & Row, 2010) has been prompted by the applicability of 'halogen bonds' in crystal engineering (Saha *et al.*, 2006). A contour map of the Laplacian of the electron density in the region of the Cl···Cl bond path is shown in Fig. 6, where a slight polar flattening can be observed in the electron distribution around

Figure 5
Symmetrically non-equivalent intermolecular bond paths linking a reference molecule (solid grey) with its nearest neighbors. (3,−1) critical points are drawn as small circles. (a) and (b) are two independent arbitrary views chosen for the sake of clarity. Roman numbers label the symmetry operation each pair is generated by (see Table 4).

both Cl atoms. The fact that the electron-deficient region in one of the Cl atoms and the electron concentration in the other do not just face each other can in part be attributed to the competition of the S atom. However, the Cl···Cl interaction in Cl(O)SEt would not seem to match any of the two models usually discussed when only halogen···halogen interactions are considered (Hathwar & Row, 2010). A Cl···Cl distance of 3.68 Å would be more consistent with a Nyburg-type interaction (Nyburg & Wong-Ng, 1979a,b), although Bui et al. (2009) have recently reported a Williams type (Williams & Hsu, 1985) interaction with a Cl···Cl distance of ca 3.65 Å.

The Cl···S^{vi}, C1···S^{vi} and H$_{et}$···Cl^v interactions (see Figs. S1 and S2 of the supplementary material for the corresponding Laplacian maps) are comparable in strength with the Cl···Cl contact. Not surprisingly, S and Cl are involved in several interactions each.
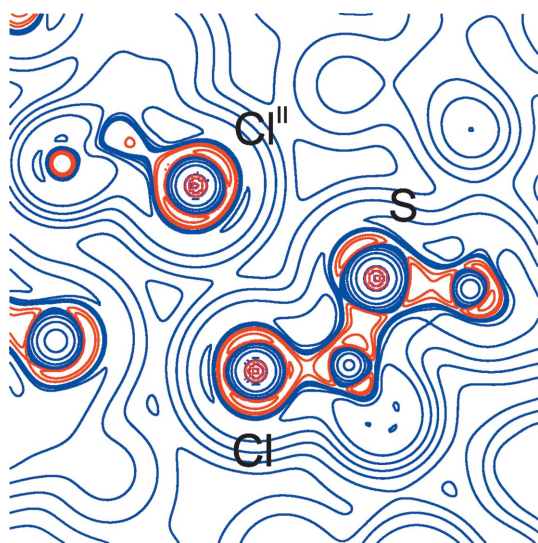
It should also be noticed that the bond path linking the O atom with a methyl H atom is markedly bent. Indeed, its major part lies around a line through H and the midpoint of the C=O bond, and only near this bond does it suddenly deviate to the oxygen. On the basis of this behavior this interaction can be characterized as a C—H···π interaction (Rozas et al., 1997; Tang & Cui, 1996; Novoa & Mota, 2000).

It could be said that the H$_3$C···Cl and H···H bond paths make little chemical sense and could be suspected of being artifacts of the charge-density model. To test the possibility of a basis-set dependence of those results we investigated a supramolecular calculation on a five-molecule cluster that contains the involved attractor pairs (namely the central molecule and those generated by the operations $-1-x, -\frac{1}{2}+y, \frac{1}{2}-z$; $x, -1+y, z$; $x, -\frac{1}{2}-y, -\frac{1}{2}+z$ and $x, \frac{1}{2}-y, -\frac{1}{2}+z$). At the B3LYP/6-31G** level the resulting bond paths are completely equivalent to those found in the crystal, as they are when 6-31+G** and 6-31++G** bases are used. At the B3LYP/6-311G** level, however, no H$_3$C···Cl bond path is found, confirming a basis set dependence in this particular case. Instead, H···H bond paths in this specific cluster are found independently of the basis set used.

The topological parameters of the covalent bonds for the in-crystal molecule and for the isolated molecule with the crystal geometry are reported in Table S1 of the supplementary material. From those data it can be concluded that, as expected, intermolecular interactions induce only minor changes in covalent bonds. The only remarkable feature is the large value of the ellipticity of the S—C1 bond ($\varepsilon > 0.3$). This fact would be indicative of a partial double-bond character of that bond, which length is consistently closer to the typical value of a S=C double bond than to that of a single C—S one (see Table 3).

4. Conclusions

The molecular structure of crystalline ClC(O)SCH$_2$CH$_3$ was obtained by low-temperature X-ray diffraction. The joint analysis of experimental and theoretical data based on NBO population analysis allowed us to understand in detail the conformational and structural features of the ClC(O)SY moiety, showing a clear dependence on the electronegativity of the Y group mainly through the influence on the donor–acceptor interactions. Electronic interactions between lone pairs of sulfur and antibonding orbitals of the ClC(O)S— moiety, especially the mesomeric and anomeric effects, were analyzed. These interactions are stronger in ClC(O)SCH$_2$CH$_3$ than in related molecules, producing a notable lengthening of the C=O bond. On the other hand, angle contractions on the

Figure 6
Laplacian (e Å^{-5}) map in the S—Cl···Cl^{ii} plane. Positive contours (blue): geometrical progression (0.024, 0.048, ..., 12) with the addition of 48, 193, 771, 3085. Negative contours (red): −4, −48, y − 120.

Lucas Rodríguez Pirani et al. · Conformational preference of chlorothioformate species **355**

research papers

planar thiocarbonate group of crystalline $ClC(O)SCH_2CH_3$ are observed, a tendency which could be related to a stronger repulsive steric interaction arising from the effective radius of the non-bonded orbital occupied by lone-pair electrons formally located around the S atom.

A topological analysis of the crystal electron density obtained from a quantum periodic calculation allowed the characterization of a network of medium–weak to weak intermolecular interactions, with a dominant $C-H\cdots O$ hydrogen bond and a $Cl\cdots Cl$ interaction playing a relevant role.

References

Bader, R. F. W. (1990). *Atoms in Molecules: A Quantum Theory.* Oxford: Clarendon Press.
Blessing, R. H. (1995). *Acta Cryst.* A**51**, 33–38.
Bohn, R. K. & Wiberg, K. B. (1999). *Theor. Chem. Acc.* **102**, 272–278.
Bondi, A. (1964). *J. Phys. Chem.* **68**, 441–451.
Brodalla, D., Mootz, D., Boese, R. & Osswald, W. (1985). *J. Appl. Cryst.* **18**, 316–319.
Bui, T. T. T., Dahaoui, S., Lecomte, C., Desiraju, G. R. & Espinosa, E. (2009). *Angew. Chem. Int. Ed.* **48**, 3838–3841.
Castro, E. A., Aliaga, M., Gazitúa, M. & Santos, J. G. (2006). *Tetrahedron*, **62**, 4863–4869.
Desiraju, G. R. (2007). *Angew. Chem. Int. Ed.* **46**, 8342–8356.
Dovesi, R., Orlando, R., Civalleri, B., Roetti, C., Saunders, V. R. & Zicovich-Wilson, C. M. (2005). *Z. Kristallogr.* **220**, 571–573.
Dovesi, R., Saunders, V. R., Roetti, C., Orlando, R., Zicovich-Wilson, C. M., Pascale, F., Civalleri, B., Doll, K., Harrison, N. M., Bush, I. J., D'Arco, Ph. & Llunell, M. (2009). *CRYSTAL*09 User's Manual. University of Torino, Italy.
Durig, J. R. & Griffin, M. G. (1977). *J. Mol. Spectrosc.* **64**, 252–266.
Erben, M. F., Boese, R., Willner, H. & Della Védova, C. O. (2007). *Eur. J. Org. Chem.* **29**, 4917–4926.
Erben, M. F., Della Védova, C. O., Boese, R., Willner, H. & Oberhammer, H. (2004). *J. Phys. Chem. A*, **108**, 699–706.
Erben, M. F., Della Védova, C. O., Romano, R. M., Boese, R., Oberhammer, H., Willner, H. & Sala, O. (2002). *Inorg. Chem.* **41**, 1064–1071.
Erben, M. F., Della Védova, C. O., Willner, H., Trautner, F., Oberhammer, H. & Boese, R. (2005). *Inorg. Chem.* **44**, 7070–7077.
Espinosa, E., Souhassou, M., Lachekar, H. & Lecomte, C. (1999). *Acta Cryst.* B**55**, 563–572.
Fiske, M. A., Bylund, W. E., Holubowitch, N. E. & Abelt, C. J. (2006). *Synthesis*, **14**, 2097–2099.
Frisch, M. J. *et al.* (2004). *GAUSSIAN*03, Revision C.02. *GAUSSIAN* Inc., Wallingford, CT, USA.
Gatti, C. (1999). *TOPOND*98 User's Manual. CNR-ISTM, Milano, Italy.
Gillespie, R. J., Robinson, E. A. & Pilmé, J. (2010). *Chem. Eur. J.* **16**, 3663–3675.
Gobbato, K. I., Mack, H.-G., Oberhammer, H., Ulic, S. E., Della Védova, C. O. & Willner, H. (1997). *J. Phys. Chem. A*, **101**, 2173–2177.
Hathwar, V. R. & Row, T. N. G. (2010). *J. Phys. Chem. A*, **114**, 13434–13441.

Kevill, D. N. & D'Souza, M. J. (1998). *J. Org. Chem.* **63**, 2120–2124.
Kirby, A. J. (1983). *The Anomeric Effect and Related Stereoelectronic Effects at Oxygen*, p. 149. Berlin: Springer-Verlag.
Lestard, M. E., Tuttolomondo, M. E., Wann, D. A., Robertson, H. E., Rankin, D. W. & Ben Altabef, A. (2009). *J. Chem. Phys.* **131**, 214303.
Matta, C. F. & Boyd, R. J. (2007). Editors. *The Quantum Theory of Atoms in Molecules: From Solid State to DNA and Drug Design*, edited by C. F. Matta & R. J. Boyd. Weinheim: Wiley-VCH.
Mirsky, K. & Cohen, M. D. (1978). *Chem. Phys.* **28**, 193–204.
Nayak, S. K., Prathapa, S. J. & Row, T. N. G. (2009). *J. Mol. Struct.* **935**, 156–160.
Novoa, J. J. & Mota, F. (2000). *Chem. Phys. Lett.* **318**, 345–354.
Nyburg, S. C. & Wong-Ng, W. (1979a). *Inorg. Chem.* **18**, 2790–2791.
Nyburg, S. C. & Wong-Ng, W. (1979b). *Proc. R. Soc. London Ser. A*, **367**, 29–45.
O'Gorman, J. M., Shand, W. & Schomaker, V. (1950). *J. Chem. Phys.* **72**, 4222–4228.
Popelier, P. (2000). *Atoms in Molecules: An Introduction.* Harlow: Prentice Hall.
Reed, A. E., Curtiss, L. A. & Weinhold, F. (1988). *Chem. Rev.* **88**, 899–926.
Riveros, J. M. & Wilson, E. B. (1967). *J. Chem. Phys.* **46**, 4605.
Romano, R. M., Della Védova, C. O. & Boese, R. (1999). *J. Mol. Struct.* **513**, 101–108.
Romano, R. M., Della Védova, C. O. & Downs, A. J. (2004). *J. Phys. Chem. A*, **108**, 7179–7187.
Romano, R. M., Della Védova, C. O., Downs, A. J., Oberhammer, H. & Parsons, S. (2001). *J. Am. Chem. Soc.* **123**, 12623–12631.
Romano, R. M., Della Védova, C. O., Downs, A. J., Parson, S. & Smith, C. (2003). *New J. Chem.* **27**, 514–519.
Rozas, I., Alkorta, I. & Elguero, J. (1997). *J. Phys. Chem. A*, **101**, 9457–9463.
Saha, B. K., Nangia, A. & Nicoud, J.-F. (2006). *Cryst. Growth Des.* **6**, 1278–1281.
Salomon, C. J. & Breuer, E. (2000). *Synlett*, **6**, 815–816.
Sarma, J. A. R. P. & Desiraju, G. R. (1986). *Acc. Chem. Res.* **19**, 222–228.
Saunders, V. R., Dovesi, R., Roetti, C., Causà, M., Harrison, N. M., Orlando, R. & Zicovich-Wilson, C. M. (1998). *CRYSTAL*98 User's Manual. University of Torino, Italy.
Sheldrick, G. M. (2008). *Acta Cryst.* A**64**, 112–122.
Shen, Q. & Hagen, K. (1985). *J. Mol. Struct.* **128**, 41–48.
Shen, Q., Krisak, R. & Hagen, K. (1995). *J. Mol. Struct.* **346**, 13–19.
Sitzmann, M. E. & Gilligan, W. H. (1985). *J. Org. Chem.* **50**, 5879–5881.
Stryer, L. (1995). *Biochemistry*, 4th ed., p. 298. New York: W. H. Freeman and Co.
Tang, T. H. & Cui, Y. P. (1996). *Can. J. Chem.* **74**, 1162–1170.
Tobón, Y. A., Di Loreto, H. E., Della Védova, C. O. & Romano, R. M. (2008). *J. Mol. Struct.* **881**, 139–145.
True, N. S. & Bohn, R. K. (1976). *J. Am. Chem. Soc.* **76**, 1188–1194.
True, N. S., Silva, C. J. & Bohn, R. K. (1981). *J. Phys. Chem.* **85**, 1132–1137.
Ulic, S. E., Coyanis, E. M., Romano, R. M. & Della Védova, C. O. (1998). *Spectrochim. Acta A*, **54**, 695–705.
Ulic, S. E., Hermann, A. & Della Védova, C. O. (2002). *J. Mol. Struct.* **641**, 233–242.
Vallejos, S. T., Erben, M. F., Willner, H., Boese, R. & Védova, C. O. (2007). *J. Org. Chem.* **72**, 9074–9080.
Vledder, H. J., Mijlhoff, F. C., Leyte, J. C. & Romers, C. (1971). *J. Mol. Struct.* **7**, 421–429.
Williams, D. E. & Hsu, L.-Y. (1985). *Acta Cryst.* A**41**, 296–301.
Yang, W. & Drueckhammer, D. G. (2001). *J. Am. Chem. Soc.* **123**, 11004–11009.
Yen, J. H., Srinivas, V. R. & Smith, G. S. (2005). *Encyclopedia of Chemical Processing*, pp. 3089–3099. Boca Raton: CRC Press.
Zaim, Ö. (1999). *Tetrahedron Lett.* **40**, 8059–8062.